Computers and Electronics in Agriculture 220 (2024) 108899

Contents lists available at ScienceDirect

Computers and Electronics in Agriculture

journal homepage: www.elsevier.com/locate/compag

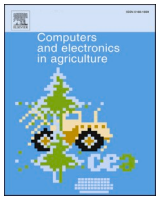

Developing remote sensing- and crop model-based methods to optimize nitrogen management in rice fields

Dong Wang [a,b,*], Paul C. Struik [a], Lei Liang [b], Xinyou Yin [a,*]

[a] Centre for Crop Systems Analysis, Department of Plant Sciences, Wageningen University & Research, P.O. Box 430, 6700 AK Wageningen, the Netherlands
[b] Shanghai Lankuaikei Technology Development Co. Ltd., No. 888 Huanhu West 2nd Road, Pudong New District, Shanghai, China

ARTICLE INFO

Keywords:
Crop model
Remote sensing
Nitrogen management
Smart farming
Sustainable agricultural production

ABSTRACT

Physiological principles-based crop modelling and *in situ* sensor technology provide opportunities for smart nitrogen (N) management for sustainable agricultural production. We propose two N-management optimization methods, in which the mathematical 'bisection algorithm' is combined either with the crop modelling (CM method) or with an integrated remote sensing-crop modelling by data assimilation (RSCM method). Data collected from a field experiment of rice with six N treatments (each with four times of topdressing) were used to illustrate the methods, where the first two N topdressings (N_{top}) were applied as in the experiment while the last two N_{top} were optimized. The two methods were compared with three reference methods: farmer practice optimized by the yield response curve (FP_{opt}), and the Sufficiency Index- or Response Index-based remote sensing (RS) methods. Crop growth and yields using N applications from these reference methods were also simulated by the same crop model. Compared with FP_{opt}, the sum of the optimized last two N_{top} of the CM method on average decreased by 37.9%, while that of the RSCM method decreased by 61.2%. The methods of CM, RSCM and RS decreased the simulated yield by 0.9%, 1.2%, and 4.4%, respectively, while they increased the profit by 2.8%, 4.4%, and −0.4%, respectively, compared with FP_{opt}. The CM method relying on crop physiological principles tended to perform better than the methods of FP_{opt} and RS in optimizing in-season N application, while the RSCM method further benefited from assimilating data from *in situ* remote sensing information into the CM framework, thereby potentially best suiting to guide smart fertilizer management.

1. Introduction

Productivity of cereal crops in China has doubled, while chemical fertilizer application increased by threefold, over the past forty years (National Bureau of Statistics of China, http://data.stats.gov.cn). China's agriculture is dominated by smallholder farms, and nitrogen (N) fertilizers tend to be over-used in farmer practice (FP) (Cui et al., 2018; Moebius-Clune et al., 2013). While about 45 % of current grain yield productivity can be attributed to this high N input (Yu et al., 2019), the FP also caused severe environmental issues, including leaching, eutrophication, greenhouse gas emission, and potential human health hazards (e.g., Cui et al. (2018); Zhang et al. (2013)). The Chinese government has invested 10.7 billion dollars from 2007 to 2022 to control the eutrophication of Taihu (Taihu Basin Authority of Ministry of Water Resources, http://www.tba.gov.cn). For both economic and environmental reasons, there is a need for the precise field N management that synchronizes soil N supply and crop demand (Cui et al., 2010). However, considering the spatial and temporal variability in soil properties and crop needs (Pierce and Nowak, 1999), the optimum N of whole-season total N application (N_{tot}) and in-season N topdressing (N_{top}) varies (Dumont et al., 2016; Mamo et al., 2003). This poses a great challenge for the sustainable agricultural production (Moebius-Clune et al., 2013).

Production functions have been commonly adopted for fitting the yield response curve showing the relationship of yield versus N_{tot} to determine the optimal N_{tot} (e.g., Cui et al. (2010); Fageria and Baligar (2005)). However, nitrogen fertilizer management, particular the appropriate rate and timing of application, is an important factor for the change of soil N in crop root zones (Dinnes et al., 2002). The so-called *yield goal method* can help to determine the whole-season N_{tot} and in-season N_{top} based on the soil N cycle and plant N uptake (Stanford, 1973). The N_{tot} is divided between two or three applications within the growing season, with the optimal N rate for the basal or N_{top} being

* Corresponding authors at: Centre for Crop Systems Analysis, Department of Plant Sciences, Wageningen University & Research, P.O. Box 430, 6700 AK Wageningen, the Netherlands.
E-mail addresses: dong.wang@wur.nl (D. Wang), xinyou.yin@wur.nl (X. Yin).

https://doi.org/10.1016/j.compag.2024.108899
Received 8 September 2023; Received in revised form 25 March 2024; Accepted 27 March 2024
Available online 4 April 2024

determined from soil nitrate test in the root zone and a target N value of the corresponding crop growth period given the yield goal (Chen et al., 2006). Field experiments have shown that applying this strategy for the wheat-maize system in the North China Plain can reduce N application compared with FP without sacrificing crop yield (Chen et al., 2006; Cui et al., 2010). However, due to the unpredictability of the grain formation caused by the uncertain crop growth conditions, the yield goal might not give an optimum N rate (Lory and Scharf, 2003). Additionally, to account for the between- and within-field variability, considerable effort might be required for the destructive sampling and laboratory testing, especially when this method is applied at large scale. Moreover, due to the lack of standard soil sampling designs, including for example sampling intensity or interpolating methods, there are obstacles for creating soil nutrient maps for *in situ* management in large areas (Pierce and Nowak, 1999). Within the comparison of 31 N recommendation tools that mainly relied on a soil nitrate test, all tools failed to work as a universally reliable tool over diverse environmental conditions across eight corn belt states of the US (Ransom et al., 2020). There is a need for developing N-recommendation methods that are more responsive to soil and weather conditions (Ransom et al., 2020).

The proximal or remote sensing technologies have shown the potential for monitoring the spatial and temporal variability of crop growth for determining the *in situ* field N management (Hansen and Schjoerring, 2003; Pierce and Nowak, 1999). With an attainable yield target and the agronomic N efficiency (AE_N), an in-season adjustment of N_{top} for rice at tillering and panicle initiation can be made by estimating leaf N status from a chlorophyll meter or a leaf color chart (Peng et al., 2010). Huang et al. (2015) guided the N_{top} for rice at the panicle initiation using satellite multispectral images, relying on the estimated N nutrition index, defined as the ratio of the actual to the critical crop aboveground N concentration. Due to the frequent cloudy weather during the growing season of rice and coarse spatial resolution of satellite remote sensing, Unmanned Aerial Vehicle-based images, especially the hyperspectral images with higher spectral resolution, are recommended (Huang et al., 2015). For instance, by applying the Unmanned Aerial Vehicle acquired multispectral images based Sufficiency Index (SI) to wheat at stem-elongating, the N_{tot} was reduced by 15.4 % and AE_N increased from 9.07 to 10.36 kg kg^{-1}, compared with the local FP (Zhang et al., 2021). Similarly, Yao et al. (2012) demonstrated that the N_{tot} of rice was reduced by 33.3 % without yield loss over FP by optimizing the N_{top} at stem-elongating using the portable sensor based Response Index (RI), following the Nitrogen Fertilizer Optimization Algorithm developed by Raun et al. (2002).

Although the variance of crop growth status can be revealed by remote sensing for *in situ* N optimization, the temporally dynamic interactions of stress like N availability on crop growth and yield cannot be totally accounted for. Compared with the spatial variability in crop N requirements, the temporal variability of weather conditions is more important, and should be better managed (Miao et al., 2011). Relying on the ability of simulating the comprehensive interaction between the soil and crop processes under a given atmospheric condition (e.g., Yin and van Laar, 2005), process-based crop models have been considered as a powerful tool (Paz et al., 1999). As future weather is always uncertain, the historical weather data over a long time have been commonly utilized for crop growth simulation to optimize N_{top} (e.g., Paz et al. (1999); Wang et al., (2021a)). However, due to the gathering cost of soil data, the between- and within-field variabilities of crop growth cannot be simulated sufficiently by crop models only (Basso et al., 2007). To simulate the space–time continuum of crop production by a crop model, Paz et al. (1999) divided the field into a grid for optimizing N_{tot}, in which the crop model was separately run with calibrated soil parameters by measured yield for each grid cell. Coupling a crop model and remote sensing technologies has recently been shown to better optimize field N management. For instance, based on the remotely sensed vegetation index or yield map, a field was delineated into a few stable zones of similar crop response and the crop model DSSAT was executed with specific inputs in each of these zones (Basso et al., 2007). Instead, Baret et al. (2007) generated a map of N_{top} for a targeted field at pixel level (20 m × 20 m), based on the updated crop growth status by assimilating in-season remote sensing observations into the crop model STICS. With the improved forecasting accuracy of crop growth status, the optimized N_{top} is supposed to benefit from the integrated system as well (Baret et al., 2007). Thus, more work is needed about assimilating remote sensing information into crop models for optimizing in-season *in situ* N management (Morari et al., 2020).

In this study, methods for optimizing field N management based on remote sensing image and crop model were developed and evaluated in comparison with earlier remote sensing-based and yield response curve-based methods. Due to the great N loss potential caused by frequent irrigation, timely N management is especially important for rice, compared with other major field crops (Fageria and Baligar, 2005). Our field experiments of rice conducted in the years 2019 and 2020, reported earlier (Wang et al., 2023a, 2023b), were adopted here as a case study. The crop model GECROS was used, because of its generality and physiological robustness (Yin and van Laar, 2005) (see a brief description of the crop model GECROS in Supplement A).

2. Materials and methods

2.1. Field experiment design

Details of the experimental design were provided previously (Wang et al., 2023a, 2023b), and here, only summary information is given. The field study was conducted on a paddy field, located in Chongming, Shanghai, China (31.67 N, 121.35E), a typical site for rice cultivation in Yangtze River Delta (Fig. 1). The soil type of the experimental site was silt loam. The meteorological records of the local weather station around our experimental site were collected from the website of the China meteorological data service centre (http://data.cma.cn). Monthly average temperature and rainfall from 1989 to 2020 are shown in Fig. S1.

The N_{tot} of the local FP is 240 kg N ha^{-1} per season. To assess the optimal N_{tot}, six treatments with varied N application amounts from 0 to 320 kg N ha^{-1} were arranged, in a complete randomized block design, with three (2019) or four (2020) blocks, in which each single plot occupied an area of 180 m^2. Rice was sown with a row spacing of 20 cm and a within-row seed spacing of 2–3 cm on 14-Jun (2019) or 4-Jun (2020). The application time and amount of N were split as scheduled (Table 1). Sufficient phosphate (112.5 kg P_2O_5 ha^{-1}) and potash (112.5 kg K_2O ha^{-1}) fertilizers were applied per season, based on the local practice, to prevent phosphorus and potassium deficiencies. Other soil and crop management practices (including irrigation, and pest, weed and disease control) were the same in each plot following local standard practices.

The optimization of N_{top} was established in the field experiment in 2020. In this study, the decision date was set at two weeks after tillering. Before the decision date, half of the N_{tot} for each treatment was applied at the stages of seedling and beginning of tillering, following the field experimental design (Table 1). Thus, six treatments with the applied N varied from 0 to 160 kg N ha^{-1} were generated for evaluating N optimization methods regarding the third and fourth N_{top}. The treatments were separated into two categories of N conditions accordingly, the deficient (for the treatments with applied N before the decision date of 0, 20, 40 and 80 kg N ha^{-1}) and the sufficient (for those of 120 and 160 kg N ha^{-1}).

2.2. Field measurements and the collection of hyperspectral images

At harvest, two sampling sites were selected in each plot and their sampling areas were 2 m^2 (2019) or 4 m^2 (2020). The total fresh samples were weighed and ca. 20 % was dissected into component plant parts, including grains. The sampled grains were weighed after oven-drying at

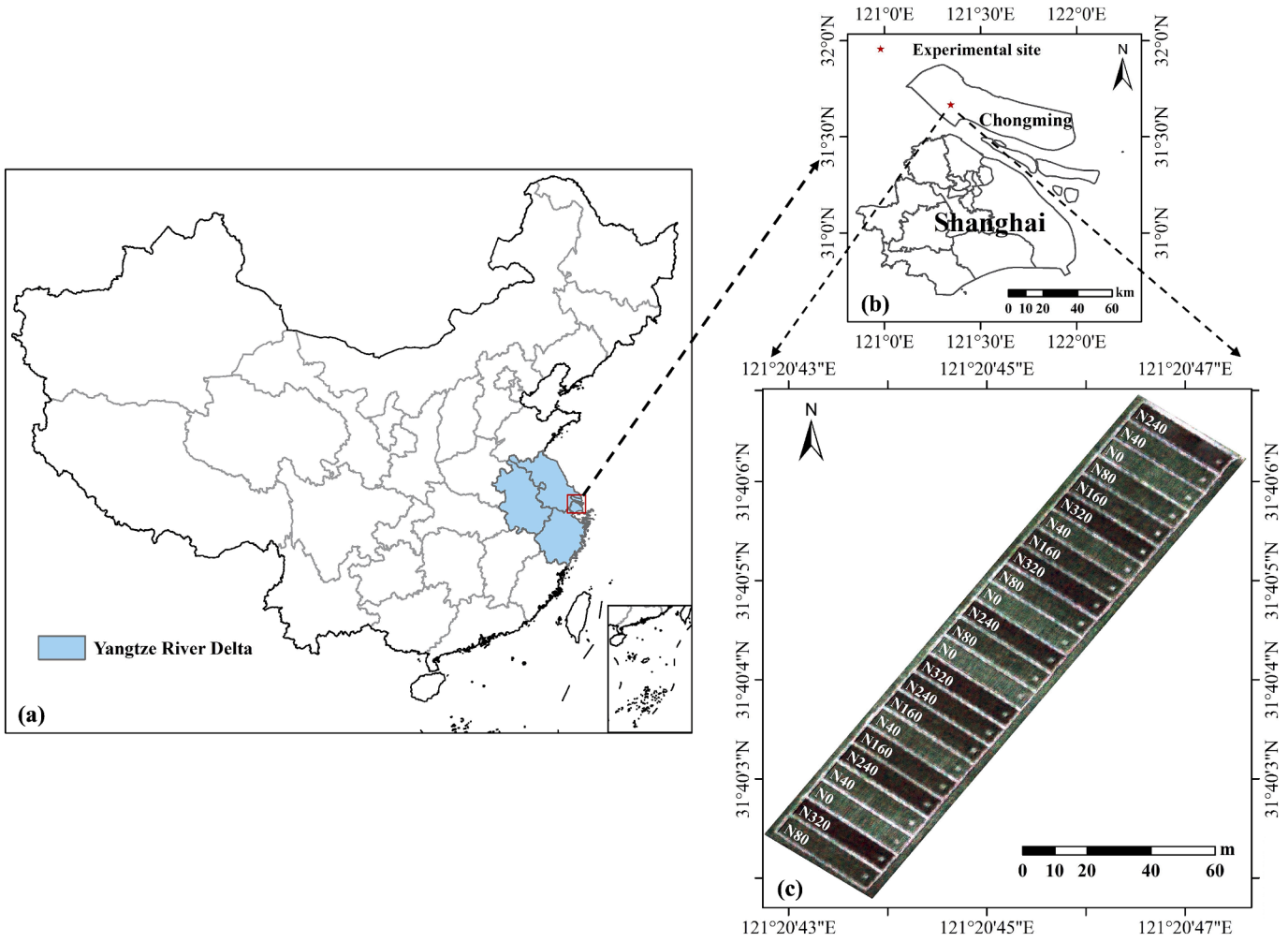

Fig. 1. Study site of the field experiment of rice (a, b). The image for field plots at the stem-elongating stage in 2020 is illustrated here (c). N0, N40, N80, N160, N240 and N320 denote different rates of nitrogen (N) application (see Table 1 for details).

Table 1
Split-applied nitrogen (N) fertilizer rates at different growth stages during the rice growing season in two experimental years following farmer practice, based on Wang et al., (2023a,2023b).

Year	Application stage	N rate (kg N ha^{-1})					
		0	40	80	160	240	320
2019	Beginning of tillering	0	16	32	64	96	128
	Two weeks after tillering	0	8	16	32	48	64
	Panicle initiation	0	10	20	40	60	80
	Two weeks after flowering	0	6	12	24	36	48
2020	Seedling	0	12	24	48	72	96
	Beginning of tillering	0	8	16	32	48	64
	Two weeks after tillering	0	8	16	32	48	64
	Panicle initiation	0	12	24	48	72	96

70 °C until constant weight. Finally, the grain yield of rice was adjusted to a moisture content of 14 %.

At the decision date of two weeks after tillering, the canopy reflectance data of the hyperspectral images were acquired. A DJI M600 PRO hexacopter (DJI, Shenzhen, China), equipped with a Cubert S185 hyperspectral snapshot camera (Cubert GmbH, Ulm, Baden-Württemberg, Germany), was flown over the experimental paddy field between 10 a.m. and 2 p.m. 125 spectral bands were captured in the range of 450–950 nm with a sampling interval of 4 nm. The spatial resolution of remote sensing images and fertilization maps was set at 1 m^2 in this study, due to the distinguished spatial variability recommended from previous studies (e.g., Solie et al., 1996).

2.3. Nitrogen optimization strategies

In this study, we proposed two methods, a crop model-based (CM) method and an integrated remote sensing-crop model (RSCM) method, to optimize N fertilization. These two methods were compared with three reference methods (two remote sensing-based (RS) methods, and yield response curve-based method), in terms of either yield or profit. Profit, P, was defined as,

$$P = yp_y - xp_x \quad (1)$$

where y and x represent the yield and N application amount, respectively, and p_y and p_x represent their prices, respectively. Other costs, like labor, fuel and machinery, are not included here. The values of p_y and p_x were from local government (https://www.shcm.gov.cn) and defined as 0.407 and 0.875 $ kg^{-1}, respectively.

Moreover, the varied N_{tot} following the fixed ratio of N partitioning from FP was also incorporated for comparison. As there was no optimization of partitioning ratios of N_{top} in FP, the amount of total N_{top}, the sum of the third and fourth N_{top}, was as same as the amount of N applied before the decision date (Table 1). Within the RS methods, as only the third N_{top} could be optimized after acquiring hyperspectral images at the decision date of two weeks after tillering, the fourth N_{top} was kept as same as that of yield response curve-based method for consistency with the limitation that the N_{tot} should not exceed the optimized N_{tot} from the

production function (see later).

2.3.1. The crop model-based optimization method

In the CM method, the N_{top} optimization was based on the crop model with a bisection algorithm (Conte and De Boor, 1965; Supplement B). While applying the method for optimizing N_{top} in the interval of the lower bound (N_{lb}) to the upper bound (N_{ub}) to maximize yield or profit, the midpoint $(N_{lb} + 2\Delta N)$ of the interval is replaced with either N_{lb} or N_{ub} that comes with lower simulated yield or profit, where ΔN is calculated as $(N_{ub} - N_{lb})/4$ (Fig. 2a). As yield always increases with an increase in N apply until the optimal N_{top} and then may slightly decrease, to reduce the required times of simulation and improve searching efficiency, the new interval can be selected by comparing the simulated yield or profit of the midpoints of candidate intervals of $[N_{lb}, N_{lb} + 2\Delta N]$ and $[N_{lb} + 2\Delta N, N_{ub}]$ (Fig. 2b).

To optimize the third and fourth N_{top} simultaneously, a double-bisection algorithm was designed as follows:

1. The amount of leftover N after the first two N_{top} was obtained according to the whole-season N_{tot} optimized from the production function for yield response curve (see later). Both the third and fourth N_{top} were varied in the initial interval of zero (lower bound, N_{lb}) to the amount of leftover N (upper bound, N_{ub}).
2. The ΔN of the third and fourth N_{top} was set to $(N_{ub,3rd} - N_{lb,3rd})/4$ and $(N_{ub,4th} - N_{lb,4th})/4$, respectively. The candidate intervals of the third N_{top} were bisected as $[N_{lb,3rd}, N_{lb,3rd} + 2\Delta N_{3rd}]$ and $[N_{lb,3rd} + 2\Delta N_{3rd}, N_{ub,3rd}]$, while that of the fourth N_{top} were $[N_{lb,4th}, N_{lb,4th} + 2\Delta N_{4th}]$ and $[N_{lb,4th} + 2\Delta N_{4th}, N_{ub,4th}]$.
3. The midpoints of candidate intervals of the third N_{top}, $(N_{lb,3rd} + \Delta N_{3rd})$ and $(N_{lb,3rd} + 3\Delta N_{3rd})$, were paired with that of the fourth N_{top}, $(N_{lb,4th} + \Delta N_{4th})$ and $(N_{lb,4th} + 3\Delta N_{4th})$. Pairs whose total amount of the third and fourth N_{top} was higher than the amount of leftover N were recognized as illegal and excluded.
4. The yields or profits were derived from the simulated crop growth by the crop model with weather data and the candidate N_{top} pairs.
5. The N_{top} pair that gave the maximum yield or profit was selected among the candidates. However, if the relative difference of yield or profit among the pairs was less than 0.1 %, the N_{top} pair with the minimal N_{tot} was selected to avoid excessive use of N.
6. The new intervals of the third and fourth N_{top} were updated to that of the selected N_{top} pair (Fig. 2b), and ΔN_{3rd} and ΔN_{4th} were updated accordingly. This narrowed down the searching ranges of the third and fourth N_{top}.
7. The procedure continued by iterating the steps from 2 to 6. When the difference between the upper and lower bounds for both third and fourth N_{top} was less than 1 kg N ha^{-1}, the iteration stopped and the midpoint of the pair was considered as the optimal N_{top} that maximized yield or profit.

For the CM method, the weather data fusion approach (Chen et al., 2020) was incorporated. Take optimizing N_{top} in 2020 for example, thirty single-year historical (1990–2019) weather files were generated and the historical daily weather data until the decision date in each weather file were replaced by the daily records in 2020. The third and fourth N_{top} of rice were optimized based on the proposed CM method with fused weather data series. Finally, the averaged N_{top} was served as the final optimized decision.

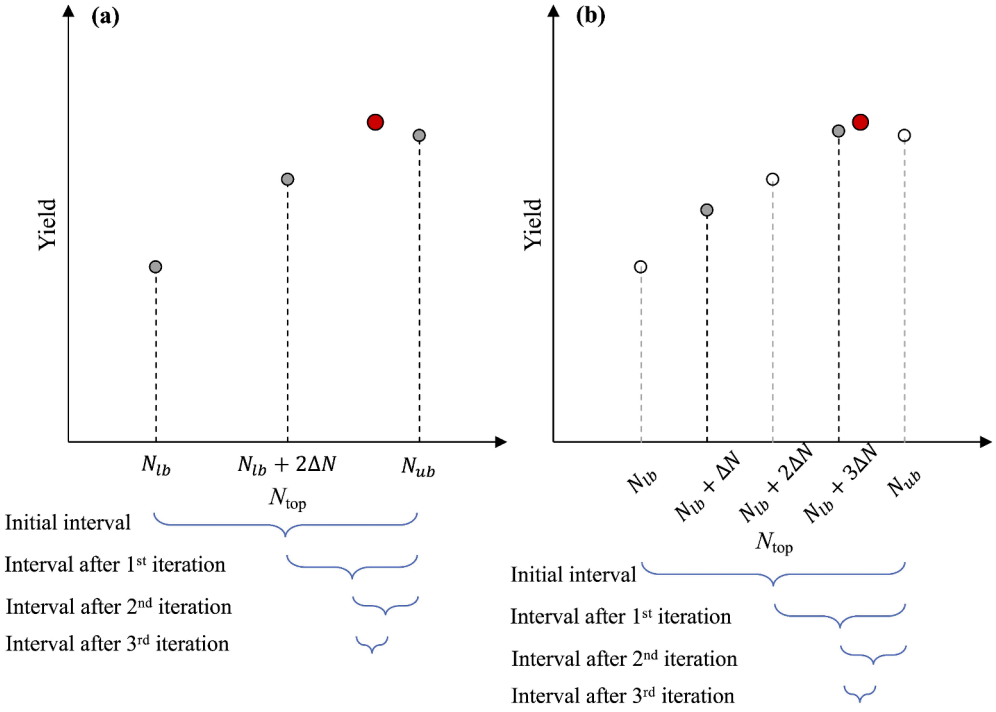

Fig. 2. Illustration of the adaptation of the bisection algorithm to optimize N topdressing (N_{top}) in our study. Panel (a) shows the original bisection method when applied in our N optimization context, where the initial interval of optimization is between lower (N_{lb}) and upper bounds (N_{ub}) and the varying step ΔN of optimization within the interval is defined as $(N_{ub} - N_{lb})/4$. Yields at N_{lb}, at N_{ub}, and at the interval midpoint $(N_{lb} + 2\Delta N)$ are calculated. Then the midpoint is set to be the new N_{lb}, generating the new interval of $[N_{lb} + 2\Delta N, N_{ub}]$ and yields at new N_{lb}, at N_{ub} and at the new midpoint are calculated. This process continues iteratively till the difference of the upper and lower bound N_{top} is less than 1 kg N ha^{-1}, and the midpoint of the final lower and upper bounds is considered as the optimal N_{top} (indicated by the red dot). Panel (b) shows the adapted procedure that improves calculation efficiency. In this procedure, the new interval is selected by comparing yields at the midpoints of candidate intervals of $[N_{lb}, N_{lb} + 2\Delta N]$ and $[N_{lb} + 2\Delta N, N_{ub}]$ (i.e. yields at only two points are calculated for each round). Then, the lower bound of the higher-yield interval of the preceding round, $N_{lb} + 2\Delta N$, is set to be the new N_{lb}, from which two new candidate intervals are formed and yields at the midpoints of these new intervals are compared. This process continues iteratively till the difference of the upper and lower bound N_{top} is less than 1 kg N ha^{-1}, and the corresponding midpoint N_{top} is considered as the optimum (indicated by the red dot).

2.3.2. The integrated remote sensing-crop model optimization method

A method of RSCM was proposed, in which the CM method (including the above-described optimization method) was further incorporated into the integrated system for crop status monitoring and data assimilation developed in our previous study (Wang et al., 2023a). Within the integrated system, Monte Carlo-based Ensemble Kalman Filter (Evensen, 1994), one of the most popular methods for data assimilation (Carrassi et al., 2018), is applied to assimilate the crop model simulations and remotely sensing observations based on their quantified uncertainties. A Markov Chain Monte Carlo approach (Vrugt et al., 2009; Schoups and Vrugt, 2010) was adopted to calibrate the uncertain parameters in crop model GECROS and estimate their posterior probability distribution functions. The uncertainties of crop growth simulations were estimated simultaneously by incorporating an assumed residual model. Remotely sensed canopy-level leaf traits, leaf weight, leaf N content and leaf area index, were predicted by a Gaussian Process Regression model (Rasmussen and Williams, 2006), with the uncertainties of remote sensing observations estimated from the model itself. The feature set combining reflectance, vegetation indices and texture information was extracted from the collected hyperspectral images for the better prediction of leaf traits (Wang et al., 2023b). While applying Ensemble Kalman filter, the procedure iteratively alternates between model forecasting and state updating. Each forecasting step produces an ensemble of different crop model simulations with uncertainties from an ensemble of parameter sets, which were sampled from the estimated posterior probability distribution functions. Each updating step uses the predicted remotely sensed observations, weighted by the estimated uncertainties from the Gaussian Process Regression model, to correct the ensemble forecast. Consequently, the crop model simulations of canopy-level leaf traits were updated directly in the integrated system and those of aboveground biomass, grain weight, aboveground N content and grain N content were updated indirectly for their better forecasting (Wang et al., 2023a).

To this end, based on the acquired hyperspectral images in 2020, the crop status at two weeks after tillering in the experimental area was updated pixel by pixel by the integrated system accordingly. The third and fourth N_{top} were optimized in a pixelated manner in the RSCM method. Like with the CM method, historical weather records after the decision date were used in the RSCM method to optimize N_{top} under different weather conditions and the averaged N_{top} map was generated as the final decision.

2.3.3. Remote sensing methods

Two remote-sensing methods are evaluated. The two methods are based on Sufficiency Index (SI) and Response Index (RI), respectively. The SI is expressed as:

$$SI = \frac{V_{sen}}{V_{ref}} \tag{2}$$

where V_{sen} and V_{ref} represent the sensed crop property and that from the referenced crop of N-rich treatments under the same measurement condition, respectively. SI ranges from zero to one; the closer SI is to one, the more sufficient the N supply is. V_{ref} in this study was from the treatment 240 kg N ha^{-1}, which is also the local FP. Following Holland and Schepers (2013), V_{sen} or V_{ref} was calculated as $(reflectance_{nir}/reflectance_{re} - 1)$, i.e. based on the reflectance of the waveband of near infrared (nir, 850 nm) and red-edge (re, 730 nm) determined from our previous study (Wang et al., 2023b), respectively.

The RS method with SI (RS_{SI}) developed by Holland and Schepers (2010) was adopted for comparison, in which the N_{top} is formed as,

$$N_{top} = \left(N_{tot,opt} - N_{PreDeci} - N_{\overline{OM}}\right)\sqrt{\frac{1 - SI}{\Delta SI\left(1 + 0.1e^{m(SI_{Threshold} - SI)}\right)}} \tag{3}$$

where $N_{tot,opt}$ is the optimal N_{tot} for maximizing yield or profit, $N_{PreDeci}$ is the amount of N applied before the decision date, and $N_{\overline{OM}}$ is the N credit for the organic matter content within the field. ΔSI is defined as the sufficiency index difference parameter and calculated as $1 - SI_0$, in which SI_0 denotes the SI when there is no N application, representing the difference between the SI of healthy plants (SI = 1.0) and those hardly able to recover by topdressing N. m and $SI_{Threshold}$ are the back-off parameters controlling the reducing rate of N_{top} for situations with reduced yield potential (i.e., plant density), which are described as the back-off rate variable and the back-off cut-on point, respectively. In this study, the $N_{tot,opt}$ was determined from the production function (see later). $N_{PreDeci}$ values for different treatments were derived from field records following Table 1. The values of ΔSI were set at 0.41, as the measured SI_0 in our field experiment was 0.59. m was set at 20, according to the results of Holland and Schepers (2010) and Zhang et al. (2021). $SI_{Threshold}$ was set at 0.59 in this study, as it is supposed to coincide with the SI_0 point (Holland and Schepers, 2010). $N_{\overline{OM}}$ was estimated to be 20–30 kg N ha^{-1} per 1 % soil organic matter (Holland and Schepers, 2013), and set to 60 kg N ha^{-1} for this study, based on the tested soil organic matter of 3 % at the experimental site.

The in-season RI, proposed by Raun et al. (2002), is equivalent to the reciprocal of SI in our context, i.e.:$RI = V_{ref}/V_{sen}$. N_{top} optimized by the RS method with RI (RS_{RI}), known as the Nitrogen Fertilizer Optimization Algorithm, is described as (Raun et al., 2002; Raun et al., 2005):

$$N_{top} = \frac{N_{grain}}{NUE} YP_0(RI - 1) \tag{4}$$

where N_{grain} represents the average N uptake (2.0 kg) per 100 kg grains for *Japonica* rice cultivars in Yangtze River Delta (Ling et al., 2005). Nitrogen use efficiency (NUE, harvested grain N (kg) per 1 kg of applied N fertilizer) is set to 0.6, as the theoretical NUE of an in-season N application is ranged from 0.5 to 0.7 (Raun et al., 2005). The prediction of yield potential with no added fertilization (YP_0, kg ha^{-1}) is followed the form of $YP_0 = aINSEY + b$, in which In-Season Estimated Yield (INSEY) is determined by dividing V_{sen} by the number of growing degree days (GDD) > 0 from emergence to sensing. The GDD is calculated as $GDD = (T_{min} + T_{max})/2 - T_b$. T_{min} and T_{max} represent the daily minimum and maximum air temperature, respectively, while T_{b} is the base temperature for phenological development and set at 8.0 °C for rice (Yin and van Laar, 2005). The potential yield with additional N fertilizer, the product of YP_0 and RI, should not exceed the maximum of field measurements (Raun et al., 2002), which is equal to 11.2 t ha^{-1} in this study. The RI is capped at 2.0 as the in-season N_{top} would unlikely lead to the potential yield two times greater than the baseline YP_0 (Raun et al., 2002).

2.3.4. Production function and yield response curve

The optimal N_{tot} in this study was defined as the N_{tot} at which the yield or profit was maximized. Here, yield response curve to N observed in our experiments was fitted to a cubic model, a simplified application of the growth functions proposed by Yin et al. (2003):

$$y = y_0 + \frac{(y_{max} - y_0)(3x_e - 2x)x^2}{x_e^3} \tag{5}$$

where y_0 denotes the value of yield when there is no N input, y_{max} denotes the maximum value of yield and x_e represents the amount of N when y_{max} is achieved. In the form of this equation, all the three parameters have a straightforward biological meaning.

The economically optimum N_{tot} is defined as the N_{tot} when the first derivative of the production function equals to the price ratio of fertilizer N to yield (e.g., Cerrato and Blackmer, 1990). Based on Eqn (1), the derivative of profit with respect to N is expressed as:

$$\frac{dP}{dx} = \frac{dy}{dx}p_y - p_x \tag{6}$$

in which $\frac{dy}{dx}$ denotes the derivative of y with respect to x (or called the marginal yield); it can be solved from Eqn (5) as $\frac{dy}{dx} = \frac{6(y_{max}-y_0)}{x_e^3}x(x_e - x)$. The highest profit achieves when $\frac{dP}{dx} = 0$. Thus, the optimal N for maximizing profit, x_p, is solved as:

$$x_p = \left(kx_e + \sqrt{(kx_e)^2 - 4k\frac{p_x}{p_y}}\right)/(2k) \quad (7)$$

where k is $\frac{6(y_{max}-y_0)}{x_e^3}$. x_p is available when $\frac{p_x}{p_y} \leq \frac{kx_e^2}{4}$.

The measured yield across varied N_{tot} in both experimental years was used to fit the yield response curve. The determined optimal N_{tot} for maximizing yield or profit was able to be used directly to optimize the FP for the corresponding target, named FP_{opt} thereafter, in which the left-over N was split-applied for the last two N_{top} with fixed partitioning ratio of FP.

2.4. Evaluation of the nitrogen optimization methods

The above five methods were applied for optimizing the last two N_{top} based on our field experiment in 2020. The crop growth with the applied first two N_{top} was simulated and updated at two weeks after tillering in 2020 based on the integrated system (described in Section 2.3.2). The last two N_{top} optimized from different methods was fertilized in the forecast of their corresponding crop growth. Based on the simulated crop growth with actual weather data, the performance of the obtained N_{top} from different strategies was evaluated by yield, profit and AE_N. AE_N was calculated as:

$$AE_N = (y - y_0)/N_{tot} \quad (8)$$

3. Results

3.1. Field nitrogen optimization based on yield response curve

The yield response to N_{tot} is shown in Fig. 3. Measured yield in both experimental years increased significantly ($P < 0.05$) from no N input until N_{tot} reached 240 kg N ha^{-1} (Fig. 3a). Yield with N_{tot} at 320 kg N ha^{-1} decreased by 0.16 % (2019) and 1.89 % (2020), compared with that at 240 kg N ha^{-1}. As fitted curves for individual years of 2019 and 2020 did not differ significantly ($P > 0.05$), a general yield response curve was generated using the pooled data (Fig. 3b). Derived from the cubic yield response model, the optimal N_{tot} for maximizing yield was 282.5 kg N ha^{-1}, located in the indicated range of optimal N_{tot} (Fig. 3). Based on Eqn (7), the optimal N_{tot} for maximizing profit was calculated as 273.3 kg N ha^{-1}, which was slightly lower than that for yield (Fig. 3b).

3.2. Topdressing nitrogen based on the remote sensing methods

The maps of N_{top} optimized by the RS methods were generated based on the SI or RI map (Fig. 4). As described in the RS_{SI} method, the optimized N_{top} targeting at maximizing yield and profit changed not only with the levels of SI, but also with the levels of applied N before the decision date (Fig. S2). Due to the slight differences between the optimized N_{tot} for yield and profit, the optimized N_{top} for yield and profit changed accordingly (Fig. 4b-c, S2). Regarding the RS_{RI} method, as it recommends N just based on the potential yield (Fig. S3), only the objective of maximizing yield was included here (Fig. 4e). In N deficient treatments, the pixel-level third N_{top} optimized by the RS_{SI} method tended to be higher than that of the uniform N_{top} of FP_{opt}, while that by the RS_{RI} method tended to be lower. For instance, the third N_{top} of the RS_{SI} method for maximizing yield for N treatments with applied N in levels of 0, 20 and 40 kg N ha^{-1} increased by 66.9 %, 57.0 % and 19.0 %, respectively, and that of the RS_{RI} method on average decreased by 8.7 % (Table S1). The plot-level total amount of the last two N_{top} (hereafter referred to as total N_{top}) of the RS_{SI} method in all treatment for maximizing yield and profit decreased, compared with that of FP_{opt}, by 39.4–51.8 % and by 39.6–51.1 %, respectively (Table 2). Similarly, the total N_{top} of the RS_{RI} method for maximizing yield decreased by 42.9–61.5 % (Table 2).

3.3. Determining the optimal topdressing nitrogen with the crop model method

As the optimization of N_{top} from the CM method used historical weather records, its applicability was validated at first. Compared with using the actual weather data, simulated yield by the historical records

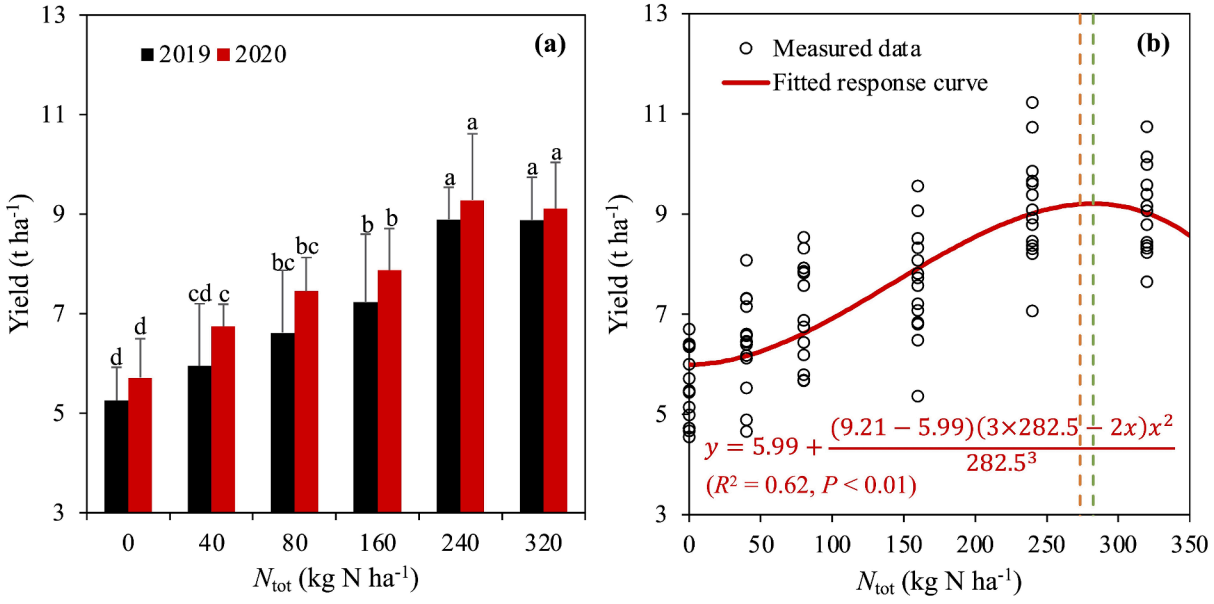

Fig. 3. Bar plots of measured yield (a) and yield response curve (b) to the varied N application amount (N_{tot}). The error bars in panel a denote the standard deviations derived from replications. The response equation for yield in panel b was fitted by Eqn (5) to two years' data in 2019 and 2020, and the green and orange vertical lines represent the optimized N_{tot} for maximizing yield and profit, respectively.

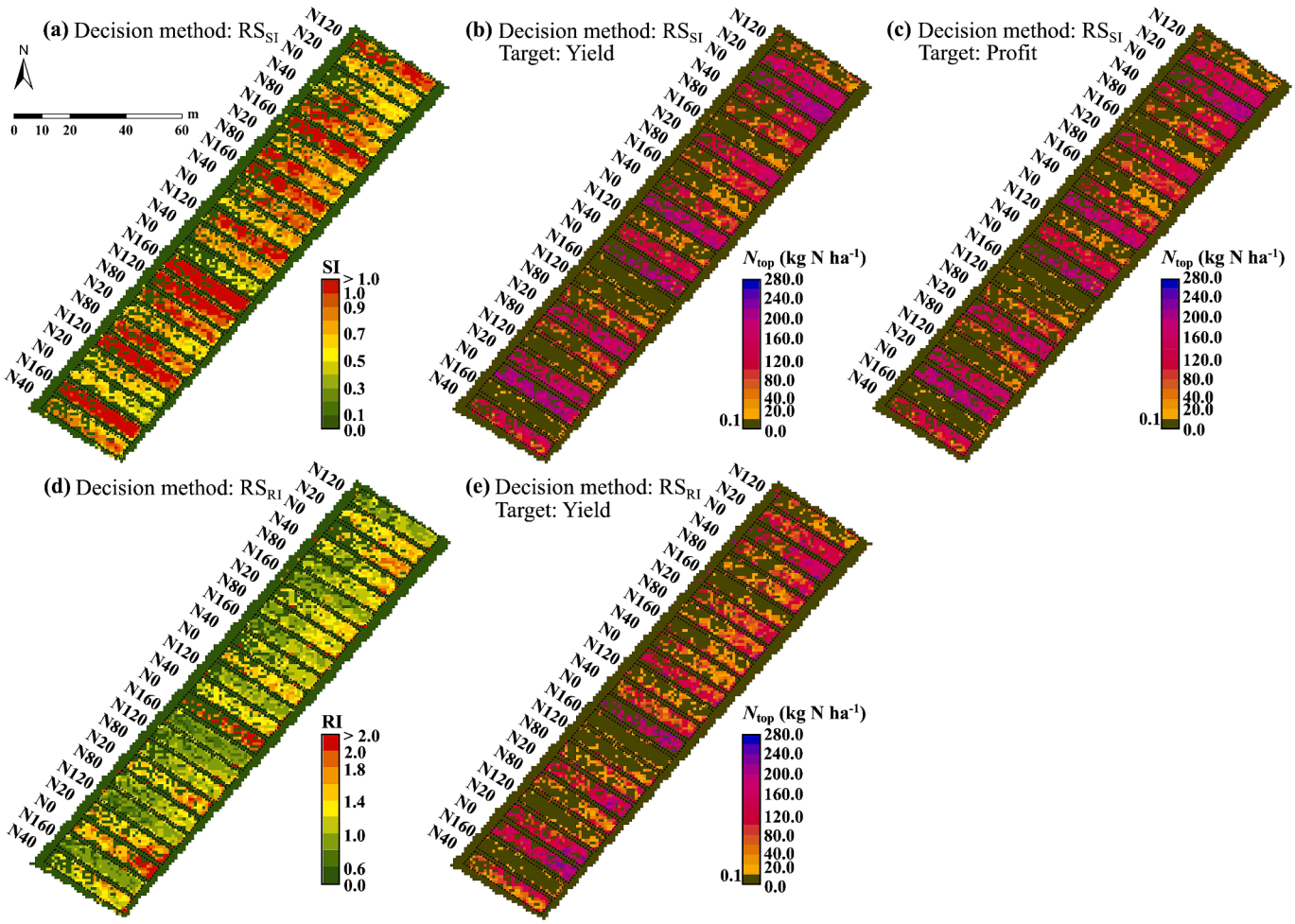

Fig. 4. Maps of Sufficiency Index (SI) (a), Response Index (RI) (d) and optimized topdressing N (N_{top}) by the method of remote sensing with SI (RS_{SI}) or RI (RS_{RI}). Within the method of RS_{SI}, N_{top} was optimized for maximizing yield (b) and profit (c), respectively. As the RS_{RI} method recommends N just based on the potential yield, the objective of maximizing yield was only included (e). N0, N20, N40, N80, N120 and N160 denote varied N rates applied before the decision (the decision date was set at two weeks after tillering, see the text). The dotted lines within the maps depict the boundaries of experimental plots.

agreed well with the field measurements in both experimental years of 2019 and 2020 (Table S2). The response curve from the simulated yield by the model ($R^2 = 0.60$, $P < 0.01$, Fig. S4) was similar to that from the measured data shown in Fig. 3b. The amount of total N_{top} of the CM method was consistently decreased in different N treatments and the decrease for maximizing yield varied from 22.4 % to 54.3 % and that for maximizing profit was from 27.6 % to 55.6 %, compared with FP_{opt} (Table 2). Similar to FP, the partitioning ratio of the third N_{top} in FP_{opt} was fixed at 40 % of the total N_{top}, while that of the CM method increased to ca. 80 % and tended to be increased with the decrease of applied N before (Table 2). Compared with FP_{opt}, the third N_{top} of different treatments optimized by the CM method increased by −5.1 % to 48.9 %, while the fourth N_{top} decreased by 65.4 % to 89.2 % (Table 2).

3.4. Optimization of topdressing nitrogen by the method of remote sensing-crop model

The maps of N_{top} optimized by the integrated method of RSCM targeting at maximizing yield and profit were generated, based on updated crop growth status using the integrated system for crop status monitor and forecast (Fig. 5). Due to the difference between the optimized N_{tot} for yield and profit, like with the method of CM, the optimized third and fourth N_{top} of RSCM for yield tended to be slightly higher than that for profit in both pixel- and plot-level (Tables 2, S1). Taking the N sufficient treatment with the 120 kg N ha^{-1} applied as an example, ca. 70 % pixels of the optimized third N_{top} for maximizing yield were in the range from 85 to 100 kg N ha^{-1}, while that for maximizing profit ranged from 75 to 90 kg N ha^{-1} (Fig. 6). The total N_{top} of RSCM in both pixel- and plot-level was lower than that of RS, and like with the CM method, more N tended to be allocated to the third N_{top} (Tables 2, S1). Compared with the CM method, benefiting from the *in situ* crop growth status, the averaged pixel-level total N_{top} of different treatments optimized by the RSCM method decreased by 4.6–13.9 % (Table S1). Relying on the *in situ* optimization, the plot-level total N_{top} of RSCM further decreased, by 49.7–77.2 %, compared with FP_{opt} (Table 2).

3.5. Performance evaluation of optimized field nitrogen

Yield maps of the different N_{top} strategies were simulated using the actual weather data (Fig. 7), although the simulated yield tended to be higher than the measurements (Fig. S4). Even though the AE_N increased while decreasing N_{tot} to 40 kg N ha^{-1} following the strategy of FP, the yield and profit decreased greatly (Table 3). The method of FP_{opt} achieved the highest yield among the N optimization strategies, with the cost of the highest N_{top} and lowest AE_N (Tables 2, 3). Compared with FP_{opt}, in N deficient treatments for maximizing yield or profit, the simulated yield of the methods of CM and RSCM decreased by 0.1 % to 1.1 % and 0.2 to 1.4 %, respectively (Table 3), while their profit increased by 1.1 % to 9.4 % and 2.3 % to 13.2 %, respectively, due to the saved N (Table 3). As for the sufficient N treatment with 160 kg N ha^{-1}

Table 2
The plot-level averaged topdressing N (N_{top}, kg N ha^{-1}) in different treatments of levels of N applied before the decision date ($N_{PreDeci}$)[a]. The N_{top} for maximizing yield or profit was optimized from different strategies, the farmer practice (FP), the optimized farmer practice (FP_{opt}), the method of remote sensing with Sufficiency Index (RS_{SI}), the method of remote sensing with Response Index (RS_{RI}), the method of crop model (CM), and the integrated method of remote sensing-crop model (RSCM).

Target	$N_{PreDeci}$	Total N_{top}						Third N_{top}						Fourth N_{top}					
		FP	FP_{opt}	RS_{SI}	RS_{RI}	CM	RSCM	FP	FP_{opt}	RS_{SI}	RS_{RI}	CM	RSCM	FP	FP_{opt}	RS_{SI}	RS_{RI}	CM	RSCM
Yield	0.0	0.0	282.5	147.4	115.8	129.1	67.1	0.0	113.0	103.6	69.4	110.0	57.8	0.0	169.5	43.8	46.5	19.1	9.3
	20.0	20.0	262.5	159.0	118.9	152.1	90.1	8.0	105.0	106.6	64.1	125.1	75.6	12.0	157.5	52.4	54.8	27.0	14.5
	40.0	40.0	242.5	126.0	93.3	141.4	85.4	16.0	97.0	73.5	39.7	119.3	72.1	24.0	145.5	52.6	53.6	22.1	13.3
	80.0	80.0	202.5	106.4	89.5	130.3	88.3	32.0	81.0	46.4	29.8	106.3	70.0	48.0	121.5	59.9	59.7	24.0	18.3
	120.0	120.0	162.5	78.4	73.7	120.0	77.8	48.0	65.0	17.1	13.4	96.8	62.9	72.0	97.5	61.3	60.3	23.2	14.9
	160.0	160.0	122.5	70.6	70.0	95.0	61.6	64.0	49.0	7.7	9.8	69.6	44.5	96.0	73.5	62.8	60.1	25.4	17.1
Profit	0.0	–	273.3	142.3	–	121.4	62.3	–	109.3	99.4	–	103.7	53.5	–	164.0	42.9	–	17.7	8.8
	20.0	–	253.3	152.9	–	137.9	84.4	–	101.3	101.8	–	110.8	69.9	–	152.0	51.1	–	27.0	14.5
	40.0	–	233.3	120.9	–	135.7	80.9	–	93.3	69.8	–	110.5	67.0	–	140.0	51.0	–	25.2	13.9
	80.0	–	193.3	101.6	–	126.7	83.7	–	77.3	43.5	–	98.6	65.9	–	116.0	58.2	–	28.2	17.7
	120.0	–	153.3	75.0	–	110.5	71.4	–	61.3	15.6	–	88.8	55.6	–	92.0	59.4	–	21.7	15.8
	160.0	–	113.3	67.4	–	82.0	56.0	–	45.3	6.6	–	58.8	38.8	–	68.0	60.8	–	23.3	17.2

[a]The decision date was set at two weeks after tillering. Two categories of N conditions were separated, the deficient (for the treatments with the $N_{PreDeci}$ of 0, 20, 40 and 80 kg N ha^{-1}) and the sufficient (for those of 120 and 160 kg N ha^{-1}).

applied, both the simulated yield and profit of the methods of CM and RSCM decreased, but the AE_N of them for maximizing yield and profit on average increased by 9.2 % and 23.0 %, respectively (Table 3). As there was hardly N_{top} for N treatments with sufficient input, not only the simulated yield and profit but also the AE_N of RS were lower than those of RSCM (Fig. 7, Table 3). Moreover, compared with the local FP, the simulated yield and profit of FP_{opt} increased by 140 kg ha^{-1} and 20 $ ha^{-1}, respectively, but its AE_N decreased from 19.2 to 16.8 kg kg^{-1}, while the yield and profit of the methods of CM and RSCM increased by 54 and 15 kg ha^{-1} and 22 and 43 $ ha^{-1}, respectively, and their AE_N increased to 19.9 and 22.6 kg kg^{-1}, respectively (Table 3).

4. Discussion

4.1. Characteristics of in-season nitrogen topdressing from different nitrogen optimization methods

Guerrero et al. (2021) indicated that more N is suggested to be fed to the poor fertility fields and less to the rich fields. In line with the N_{top} at stem-elongating of winter wheat optimized by the RS_{SI} method (Zhang et al., 2021), our results also showed that higher N_{top} at the decision date of two weeks after tillering for rice tended to be recommended for the N deficient treatments (Table 2). Regarding the N sufficient treatments, less N was recommended by the RS methods, as SI tended to be higher than 1.0 or RI tended to be lower than 1.0 (Fig. 4). However, Huang et al. (2015) suggested that as the optimal or sufficient crop N status in the vegetative phase only indicates the N status at that particular stage, a certain amount of N fertilizer should still be recommended for the required N needs of the crop until the maturity. Our results showed that for the N sufficient treatments, compared with FP_{opt}, the third N_{top} optimized from the methods of CM and RSCM varied by 29.7 % to 48.9 % and −14.5 % to −3.2 % while that of the RS method decreased by 73.7 % to 85.5 % (Table 2).

While applying the strategy of FP_{opt}, more yield or profit can be achieved only through directly optimizing N_{tot}, in which N_{top} was adjusted with a fixed ratio of N partitioning. Like with FP and FP_{opt} in this study, the ratio of the third (mid-tillering) and fourth (panicle initiation) N_{top} is recommended as two to three (Peng et al., 2006). However, in the RS methods, for N deficient treatments, 33.3 % to 70.3 % of total N_{top} was allocated to the third N_{top}, while only 9.8 % to 21.8 % was allocated to the third N_{top} in N sufficient treatments (Table 2). Especially, the N partitioning of the methods of CM and RSCM performed consistently among different treatments and on average, 80.4 % of total N_{top} was applied in the third N_{top} (Table 2), indicating that more N should be allocated for tillering. Thus, the difference in early growth vigor of rice might be caused by the adjusted in-season N partitioning, which is always overlooked in N optimization methods with the fixed one (Peng et al., 2010).

4.2. Optimization of whole-season nitrogen application amount

By means of the production function in the form of the quadratic model, the economically optimal N_{tot} of rice along the Yangtze River Basin was determined within the range from 180 to 285 kg N ha^{-1} (Chen et al., 2011) and higher optimal N_{tot} was found in regions with better environmental conditions, like the Yangtze River Delta (Ren et al., 2022). However, it is noticeable that the identified optimal N_{tot} tends to differ between forms of production functions (Cerrato and Blackmer, 1990). For instance, in this study, the optimized N_{tot} for yield from the commonly used linear-plateau and quadratic model was 153.6 and 373.3 kg N ha^{-1}, respectively (Eqns (S1)-(S3) in Supplement C, Fig S5), while that from our cubic model was 282.5 kg N ha^{-1} (Fig. 3b). The measured data indicated that the linear plateau model overestimated yield in the section of the response curve close to the optimized N_{tot} and thus resulted in a lower optimum N_{tot}, while the quadratic model indicated an even higher optimum N_{tot} (Fig. 3a, S5), in line with the

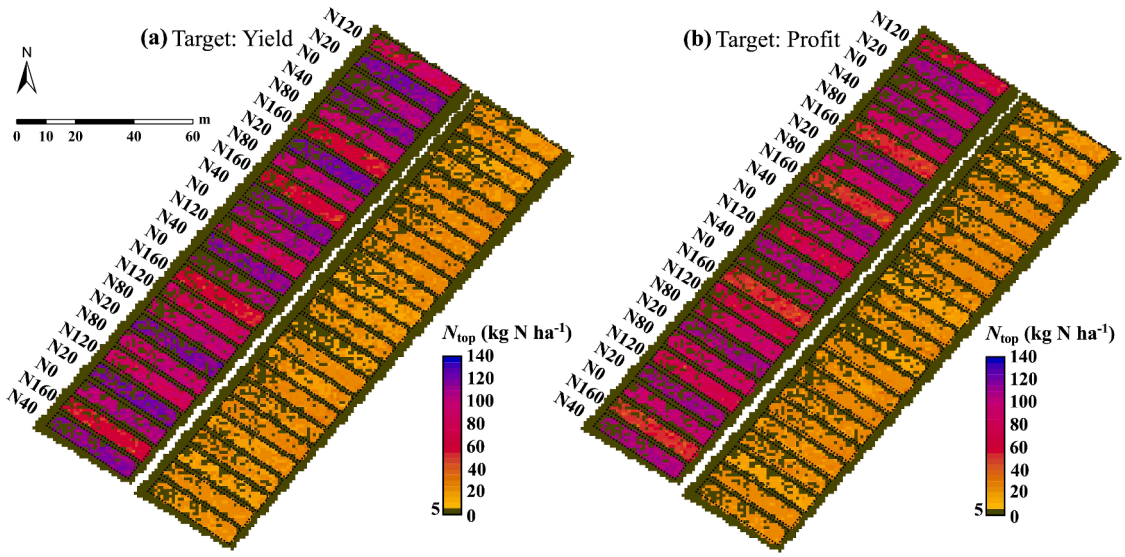

Fig. 5. Maps of optimized topdressing N (N_{top}) by the integrated method of remote sensing-crop model targeting at maximizing yield (a) and profit (b). The third and fourth N_{top} maps were shown in upper left and lower right, respectively, in each panel. N0, N20, N40, N80, N120 and N160 denote varied N rates applied before the decision (the decision date was set at two weeks after tillering, see the text). The dotted lines within the maps depict the boundaries of experimental plots.

statements of Cerrato and Blackmer (1990). Consequently, the cubic model performed better in our results (Fig. 3b).

The *in situ* N managements based on the production function are able to decrease the required N inputs, as both spatial and temporal variability are considered appropriately (Mamo et al., 2003). For instance, compared with the optimized N_{tot} (250 kg N ha^{-1}) from the production function, the optimized N_{tot} for rice from the *in situ* approaches was lower and ranged from 166 to 233 kg N ha^{-1} (Xue and Yang, 2008). Likewise, our results also showed that the N_{tot} optimized for maximizing yield for different treatments varied in the range from 115.8 to 230.6 kg N ha^{-1} (from the RS methods), from 129.1 to 255.0 kg N ha^{-1} (from the CM method) and from 67.1 to 221.6 kg N ha^{-1} (from the RSCM method), all lower than that from the production function (282.5 kg N ha^{-1}) (Table 2). Moreover, Xue and Yang (2008) recommended that not only N_{top} should be fine-tuned, but also the proportion of the basal N applied could be properly reduced. The optimization of the basal fertilizer will be incorporated together in the further study for the more efficient whole-season N arrangement.

4.3. Responses of optimized field nitrogen management to yield, profit and nitrogen use efficiency

In line with the optimized N_{top} for wheat using the method of N nutrition index (Jiang et al., 2023), our simulated results showed that the performance of the optimized N_{top} from our CM and RSCM methods was reasonable among varied N treatments of rice. Compared with FP, the yield increment of these optimization methods in N deficient treatments was similar and on average ranged from 27.5 % to 29.9 %, while the decrement of the optimized N_{tot} for the N sufficient treatment with 160 kg N ha^{-1} applied varied from 20.3 % to 32.5 % (Tables 2, 3). Compared with the CM method, the RS methods tended to save more N by the sacrifice of grain yield (Table 3). The N_{tot} of the RSCM method was able to be further decreased to a lower level than that of the RS methods, but a similar grain yield with that of CM was maintained (Tables 2, 3). The in-season N_{top} optimization considering both soil N supply and crop N demand contributes to a higher N use efficiency (Flowers et al., 2004). AE_N of different treatments with optimized N_{top} by the RSCM method increased to the range from 18.4 to 27.6 kg kg^{-1}, generally agreeing with values for the developed countries (20–25 kg kg^{-1}) (Zhang et al., 2008), while that of FP_{opt} decreased to the range from 4.8 to 18.3 kg kg^{-1} (Table 3).

In reviews of N optimization, the *in situ* optimized N seems more profitable than the uniform one (e.g., Pedersen et al. (2020)). For instance, after delineating the management zones, the profit from the *in situ* N_{top} for maize simulated by the crop model SALUS increased by 12 € ha^{-1} (13 $ ha^{-1}), compared with that from the uniform FP (Basso et al., 2016). Pedersen et al. (2021) integrated the simulated remote sensing proxies into the DAISY crop model and found that there was an expected profit increase from 6 to 29 € ha^{-1} (7 to 32 $ ha^{-1}). Our results further demonstrated the utility of the RSCM method with actual remote sensing images. Especially, compared with local FP, the profit of the methods of FP_{opt}, CM and RSCM for maximizing yield increased by 20, 22 and 43 $ ha^{-1}, respectively, although that of the RS methods decreased by 140–174 $ ha^{-1} (Table 3). Even though the profit of the method of FP_{opt} achieved the highest in N sufficient treatments, higher increment of yield and profit was achieved under N deficient conditions by the methods of CM and RSCM, in which the profit of them on average increased by 24.0 % and 26.6 %, respectively, compared with that of FP (Table 3). The results were consistent with the conclusions from Guerrero et al. (2021). However, field N under N sufficient conditions still should be optimized carefully to prevent the yield and profit loss, taking the RS methods for example (Table 3).

4.4. The applicability of crop model in field nitrogen management

Like with previous studies (Paz et al., 1999; Wang et al., 2021a), our results also showed that the crop model GECROS could be used for guiding field N management (Tables 2, 3). However, it has been claimed that the use of the crop model is limited due to the required inputs and parameters (e.g., Guerrero et al. (2021)). Thus, machine learning models have been regressed by combining soil, weather and management data with remotely sensed crop data (Wang et al., 2021b). However, the optimization of N_{top} is affected by the selection of machine learning algorithms and might fail due to the inaccurately simulated yield response (Wang et al., 2021b; Zhang et al., 2023). Meanwhile, due to the black-box nature of the machine learning algorithms, the lack of the process-based response of the crop growth hinders the in-season optimization of N_{top}, especially when considering it over a long period of time. Instead, the strength of a crop model for determining the optimal N_{tot} or N_{top} lays in interactions between genotypes, soil, weather and management and the long-term simulations under different weather conditions (Basso et al., 2016; Jiang et al., 2019).

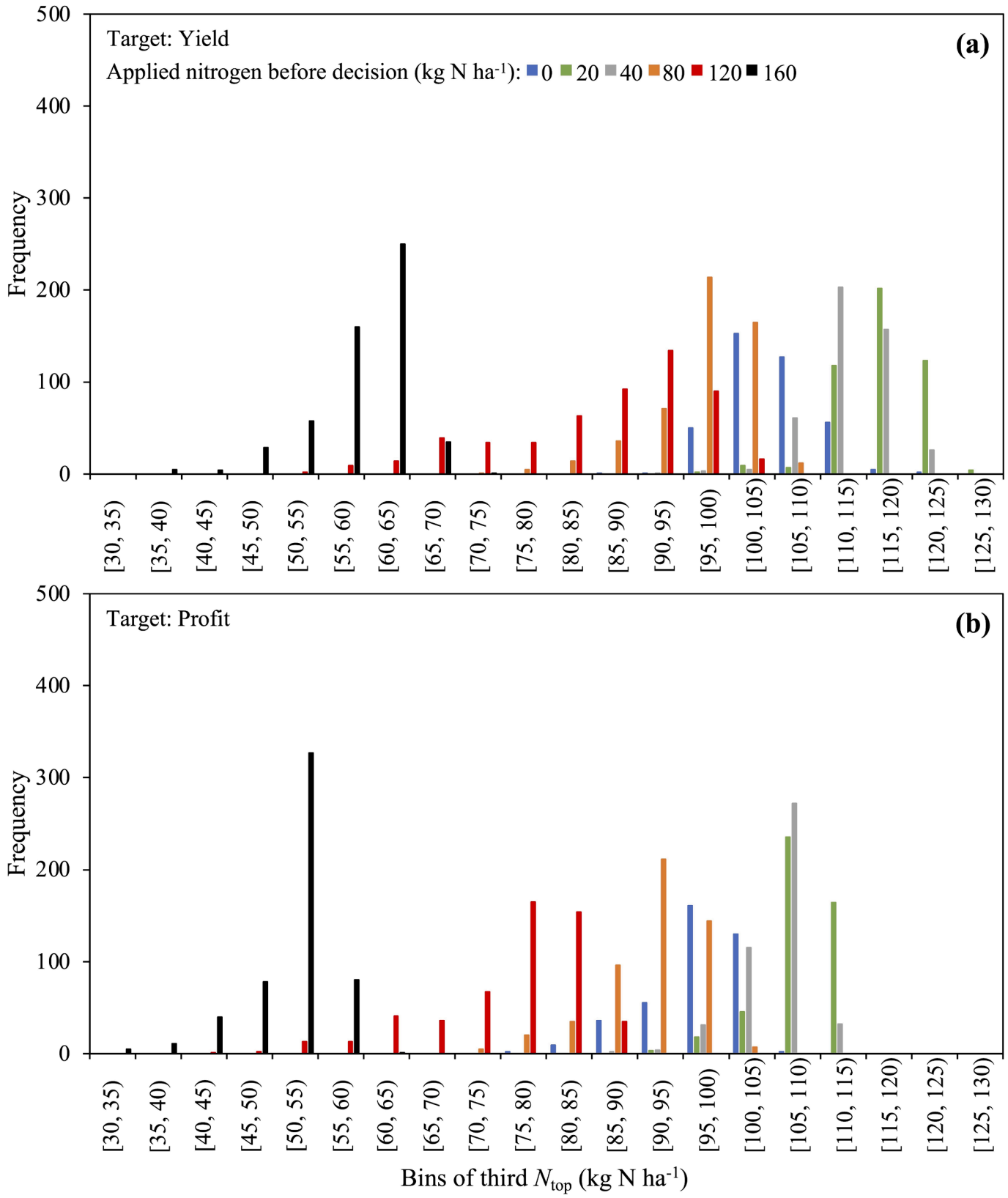

Fig. 6. The distribution of pixel-level optimized third topdressing N (N_{top}) by the method of remote sensing-crop model targeting at maximizing yield (a) and profit (b). The decision date was set at two weeks after tillering (see the text).

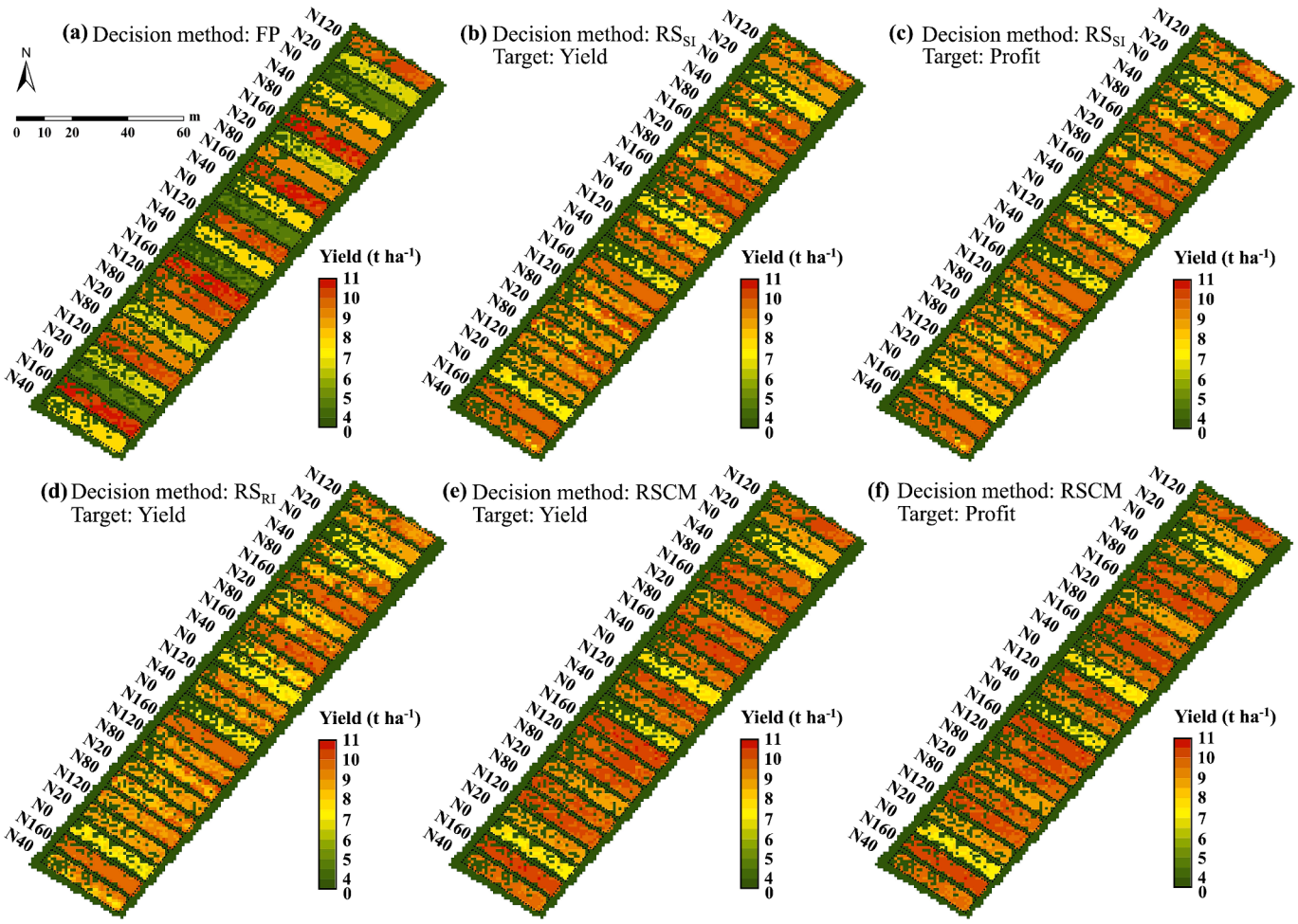

Fig. 7. Yield maps from different strategies, the farmer practice (FP) (a), the method of remote sensing with Sufficiency Index (RS_{SI}) (b, c) or Response Index (RS_{RI}) (d), and the integrated method of remote sensing-crop model (RSCM) (e, f), for optimizing topdressing N targeting at maximizing yield and profit. As the RS_{RI} method recommends N just based on the potential yield, the objective of maximizing yield was only included (d). The yield for different strategies was simulated from the crop model GECROS using actual weather data. N0, N20, N40, N80, N120 and N160 denote varied N rates applied before the decision (the decision date was set at two weeks after tillering, see the text). The dotted lines within the maps depict the boundaries of experimental plots.

Nonetheless, until now, most crop model-based approaches are still used for optimizing the averaged N rates in years or sites, rather than in-season or *in situ* (Bai and Gao, 2021). In line with previous reports for N optimization of maize at planting and V8 stage (Wang et al., 2021a), our results also showed that the weather data fusion approach enables the crop model to forecast the rice growth of entire growing season for optimizing the in-season N_{top} (Tables 2, S1). Moreover, within the integrated system of RSCM, the remote sensing observation provides the missing heterogeneously spatial information required by the crop model for the improved yield forecasting (Morari et al., 2020). Like with the results of Baret et al. (2007), relying on the RSCM method, the third and fourth N_{top} was optimized *in situ* without the cost of yield or profit loss (Table 3). Especially, compared with previous studies that optimizes N_{top} by various N levels (e.g., Baret et al. (2007); Wang et al., (2021a)), the N_{top} in this study was optimized continuously.

4.5. Prospect of the long-term application of the proposed nitrogen optimization methods

Although the N optimization methods were evaluated comprehensively by the simulations from the calibrated crop model with the actual weather data, their actual performance in real farmers' fields is of importance, especially when considering the effect of the long-term N optimization for the sustainable agricultural production. When applying these methods to real farmers' fields, the costs from information acquisition, information processing to decision implementation, need to be further included. Pedersen et al. (2020) estimated the all included costs and pointed out that it is ranged from 5 to 80 € ha^{-1} (5 to 88 $ ha^{-1}) depending on farm size. Based on the cost estimation, the varied N application from the method of RSCM in this study could be relevant on farms with 100 ha and above. By further coupling with soil information, it could be relevant on even smaller farms (Pedersen et al., 2021). Moreover, after a long-term application of the *in situ* management, the between- and within-field variability shall be diminished (Pierce and Nowak, 1999) and thus the field management can be simplified, contributing to the increase of profitability. While there are obstacles like acquiring remote sensing images and implementing *in situ* decisions, the CM method is recommended based on our results (Table 3). With the optimized long-term fertilizer management plan, severe environmental issues from over or under fertilization can be prevented for the sustainable agricultural production in the era of smarting farming (Berger et al., 2020).

5. Conclusions

In this study, two new methods, CM and RSCM, for N optimization were developed and evaluated by the simulated crop growth from the crop model GECROS in varied field N conditions. The optimized in-

Table 3
The plot-level averaged yield, profit and agronomic efficiency of N (AE_N) in different treatments of levels of N applied before the decision date ($N_{PreDeci}$) [a]. The strategies for maximizing yield or profit included the farmer practice (FP), the optimized farmer practice (FP_{opt}), the method of remote sensing with Sufficiency Index (RS_{SI}), the method of remote sensing with Response Index (RS_{RI}), the method of crop model (CM), and the integrated method of remote sensing-crop model (RSCM). The yield for different strategies was simulated from the crop model GECROS using actual weather data.

Target	$N_{PreDeci}$	Yield (t ha^{-1})						Profit ($ ha^{-1})						AE_N (kg kg^{-1})					
		FP	FP_{opt}	RS_{SI}	RS_{RI}	CM	RSCM	FP	FP_{opt}	RS_{SI}	RS_{RI}	CM	RSCM	FP	FP_{opt}	RS_{SI}	RS_{RI}	CM	RSCM
Yield	0.0	2.70	4.07	4.06	4.05	4.06	4.06	1099	1408	1525	1545	1540	1594	–	4.8	8.4	11.0	10.5	18.4
	20.0	4.25	5.79	5.78	5.63	5.77	5.75	1696	2110	2198	2169	2195	2243	38.8	10.9	17.2	21.1	17.8	27.6
	40.0	4.94	6.09	5.94	5.57	6.03	6.02	1939	2232	2273	2152	2296	2340	27.9	12.0	19.6	21.6	18.4	26.5
	80.0	6.56	7.20	6.80	6.54	7.13	7.11	2530	2685	2604	2514	2716	2747	24.1	15.9	22.0	22.6	21.0	26.2
	120.0	7.31	7.45	6.88	6.79	7.37	7.33	2766	2786	2626	2592	2788	2809	19.2	16.8	21.1	21.1	19.4	23.4
	160.0	7.86	7.87	7.44	7.40	7.76	7.72	2920	2954	2826	2809	2936	2948	16.1	18.3	20.6	20.4	19.9	22.6
Profit	0.0	–	4.07	4.06	–	4.06	4.06	–	1416	1529	–	1546	1596	–	5.0	8.7	–	11.2	19.7
	20.0	–	5.79	5.78	–	5.75	5.74	–	2118	2203	–	2203	2243	–	11.3	17.8	–	19.3	29.0
	40.0	–	6.09	5.93	–	6.03	6.01	–	2239	2274	–	2301	2339	–	12.4	20.1	–	19.0	27.3
	80.0	–	7.17	6.78	–	7.13	7.09	–	2680	2602	–	2721	2741	–	16.4	22.5	–	21.4	26.8
	120.0	–	7.43	6.87	–	7.34	7.31	–	2786	2624	–	2786	2806	–	17.3	21.4	–	20.1	24.1
	160.0	–	7.86	7.43	–	7.72	7.69	–	2961	2825	–	2930	2942	–	18.9	20.8	–	20.7	23.1

[a]The decision date was set at two weeks after tillering. Two categories of N conditions were separated, the deficient (for the treatments with the $N_{PreDeci}$ of 0, 20, 40 and 80 kg N ha^{-1}) and the sufficient (for those of 120 and 160 kg N ha^{-1}).

season N_{top} from the CM and RSCM methods was compared with that of FP_{opt} and the RS methods. Compared with FP_{opt}, although the simulated yield of the methods of CM and RSCM slightly decreased, their profit on average increased by 2.8 % and 4.4 %, respectively, and their AE_N on average increased from 13.35 kg kg^{-1} to 18.24 and 24.54 kg kg^{-1}, respectively. Compared to the local FP (240 kg N ha^{-1}), after optimizing N_{top}, the simulated yield of the methods of CM and RSCM increased by 0.6 % and 0.1 %, respectively, whereas the RS methods decreased the simulated yield by 6.0–7.2 %. In general, the developed methods of CM and RSCM benefiting from the crop physiological principles and *in situ* remote sensing information provide promising opportunities to improve the productivity, the profit and resource use efficiency for the sustainable agricultural production. However, this potential requires field experimentation or farmer's demonstration trials to verify.

CRediT authorship contribution statement

Dong Wang: Writing – review & editing, Writing – original draft, Formal analysis, Data curation, Conceptualization. **Paul C. Struik:** Writing – review & editing, Supervision, Formal analysis, Conceptualization. **Lei Liang:** Supervision, Software. **Xinyou Yin:** Writing – review & editing, Supervision, Formal analysis, Conceptualization.

Declaration of competing interest

The authors declare the following financial interests/personal relationships which may be considered as potential competing interests: Dong Wang reports a relationship with Shanghai Lankuaikei Technology Development Co. Ltd. that includes: employment. Lei Liang reports a relationship with Shanghai Lankuaikei Technology Development Co. Ltd. that includes: employment.

Data availability

The authors do not have permission to share data.

Acknowledgement

This study was partly supported by the High-tech Industry and Scientific and Technological Innovation Project of Lin-gang Special Area, Shanghai (grant number: SH-LG-GK-2020-02-19).

Appendix A. Supplementary data

Supplementary data to this article can be found online at https://doi.org/10.1016/j.compag.2024.108899.

References

Bai, Y., Gao, J., 2021. Optimization of the nitrogen fertilizer schedule of maize under drip irrigation in Jilin, China, based on DSSAT and GA. Agric. Water Manag. 244 https://doi.org/10.1016/j.agwat.2020.106555.

Baret, F., Houles, V., Guerif, M., 2007. Quantification of plant stress using remote sensing observations and crop models: the case of nitrogen management. J. Exp. Bot. 58, 869–880. https://doi.org/10.1093/jxb/erl231.

Basso, B., Bertocco, M., Sartori, L., Martin, E.C., 2007. Analyzing the effects of climate variability on spatial pattern of yield in a maize–wheat–soybean rotation. Eur. J. Agron. 26, 82–91. https://doi.org/10.1016/j.eja.2006.08.008.

Basso, B., Dumont, B., Cammarano, D., Pezzuolo, A., Marinello, F., Sartori, L., 2016. Environmental and economic benefits of variable rate nitrogen fertilization in a nitrate vulnerable zone. Sci. Total Environ. 545–546, 227–235. https://doi.org/10.1016/j.scitotenv.2015.12.104.

Berger, K., Verrelst, J., Féret, J.-B., Wang, Z., Wocher, M., Strathmann, M., Danner, M., Mauser, W., Hank, T., 2020. Crop nitrogen monitoring: Recent progress and principal developments in the context of imaging spectroscopy missions. Remote Sens. Environ. 242, 111758 https://doi.org/10.1016/j.rse.2020.111758.

Carrassi, A., Bocquet, M., Bertino, L., Evensen, G., 2018. Data assimilation in the geosciences: An overview of methods, issues, and perspectives. WIREs Clim. Change 9. https://doi.org/10.1002/wcc.535.

Cerrato, M.E., Blackmer, A.M., 1990. Comparison of models for describing; corn yield response to nitrogen fertilizer. Agron. J. 82, 138–143.

Chen, J., Huang, Y., Tang, Y., 2011. Quantifying economically and ecologically optimum nitrogen rates for rice production in south-eastern China. Agr. Ecosyst. Environ. 142, 195–204. https://doi.org/10.1016/j.agee.2011.05.005.

Chen, S., Jiang, T., Ma, H., He, C., Xu, F., Malone, R.W., Feng, H., Yu, Q., Siddique, K.H. M., Dong, Q.G., He, J., 2020. Dynamic within-season irrigation scheduling for maize production in Northwest China: A Method Based on Weather Data Fusion and yield prediction by DSSAT. Agric. For. Meteorol. 285–286 https://doi.org/10.1016/j.agrformet.2020.107928.

Chen, X., Zhang, F., Römheld, V., Horlacher, D., Schulz, R., Böning-Zilkens, M., Wang, P., Claupein, W., 2006. Synchronizing N supply from soil and fertilizer and N demand of winter wheat by an improved Nmin method. Nutr. Cycl. Agroecosyst. 74, 91–98. https://doi.org/10.1007/s10705-005-1701-9.

Conte, S.D., and De Boor, C. (1965). Elementary Numerical Analysis: An Algorithmic Approach (2nd ed.).

Cui, Z., Zhang, F., Chen, X., Dou, Z., Li, J., 2010. In-season nitrogen management strategy for winter wheat: Maximizing yields, minimizing environmental impact in an over-fertilization context. Field Crop Res 116, 140–146. https://doi.org/10.1016/j.fcr.2009.12.004.

Cui, Z., Zhang, H., Chen, X., Zhang, C., Ma, W., Huang, C., Zhang, W., Mi, G., Miao, Y., Li, X., Gao, Q., Yang, J., Wang, Z., Ye, Y., Guo, S., Lu, J., Huang, J., Lv, S., Sun, Y., Liu, Y., Peng, X., Ren, J., Li, S., Deng, X., Shi, X., Zhang, Q., Yang, Z., Tang, L., Wei, C., Jia, L., Zhang, J., He, M., Tong, Y., Tang, Q., Zhong, X., Liu, Z., Cao, N., Kou, C., Ying, H., Yin, Y., Jiao, X., Zhang, Q., Fan, M., Jiang, R., Zhang, F., Dou, Z., 2018. Pursuing sustainable productivity with millions of smallholder farmers. Nature 555, 363–366. https://doi.org/10.1038/nature25785.

Dinnes, D.L., Karlen, D.L., Jaynes, D.B., Kaspar, T.C., Hatfield, J.L., Colvin, T.S., Cambardella, C.A., 2002. Nitrogen management strategies to reduce nitrate leaching in tile-drained Midwestern soils. Agron. J. 94, 153–171.

Dumont, B., Basso, B., Bodson, B., Destain, J.P., Destain, M.F., 2016. Assessing and modeling economic and environmental impact of wheat nitrogen management in Belgium. Environ. Model. Softw. 79, 184–196. https://doi.org/10.1016/j.envsoft.2016.02.015.

Evensen, G., 1994. Sequential data assimilation with a nonlinear quasi-geostrophic model using Monte Carlo methods to forecast error statistics. J. Geophys. Res. Oceans 99, 10143–10162.

Fageria, N.K., Baligar, V.C., 2005. Enhancing Nitrogen Use Efficiency in Crop Plants. Adv. Agron. 88, 97–185. https://doi.org/10.1016/s0065-2113(05)88004-6.

Flowers, M., Weisz, R., Heiniger, R., Osmond, D., Crozier, C., 2004. In-season optimization and site-specific nitrogen management for soft red winter wheat. Agron. J. 96, 124–134.

Guerrero, A., De Neve, S., Mouazen, A.M., 2021. Data fusion approach for map-based variable-rate nitrogen fertilization in barley and wheat. Soil Tillage Res. 205, 104789 https://doi.org/10.1016/j.still.2020.104789.

Hansen, P.M., Schjoerring, J.K., 2003. Reflectance measurement of canopy biomass and nitrogen status in wheat crops using normalized difference vegetation indices and partial least squares regression. Remote Sens. Environ. 86, 542–553. https://doi.org/10.1016/s0034-4257(03)00131-7.

Holland, K.H., Schepers, J.S., 2010. Derivation of a variable rate nitrogen application model for in-season fertilization of corn. Agron. J. 102, 1415–1424. https://doi.org/10.2134/agronj2010.0015.

Holland, K.H., Schepers, J.S., 2013. Use of a virtual-reference concept to interpret active crop canopy sensor data. Precis. Agric. 14, 71–85. https://doi.org/10.1007/s11119-012-9301-6.

Huang, S., Miao, Y., Zhao, G., Yuan, F., Ma, X., Tan, C., Yu, W., Gnyp, M., Lenz-Wiedemann, V., Rascher, U., Bareth, G., 2015. Satellite remote sensing-based in-season diagnosis of rice Nitrogen Status in Northeast China. Remote Sens. (Basel) 7, 10646–10667. https://doi.org/10.3390/rs70810646.

Jiang, R., He, W., Zhou, W., Hou, Y., Yang, J.Y., He, P., 2019. Exploring management strategies to improve maize yield and nitrogen use efficiency in northeast China using the DNDC and DSSAT models. Comput. Electron. Agric. 166, 104988 https://doi.org/10.1016/j.compag.2019.104988.

Jiang, J., Wu, Y., Liu, Q., Liu, Y., Cao, Q., Tian, Y., Zhu, Y., Cao, W., Liu, X., 2023. Developing an efficiency and energy-saving nitrogen management strategy for winter wheat based on the UAV multispectral imagery and machine learning algorithm. Precis. Agric. 24, 2019–2043. https://doi.org/10.1007/s11119-023-10028-6.

Ling, Q., Zhang, H., Dai, Q., Ding, Y., Ling, L., Su, Z., Xu, M., Que, J., Wang, S., 2005. Study on precise and quantitative N application in rice (in Chinese with English abstract). Sci. Agric. Sin. 38, 2457–2467. https://doi.org/10.3321/j.issn:0578-1752.2005.12.014.

Lory, J.A., Scharf, P.C., 2003. Yield goal versus delta yield for predicting fertilizer nitrogen need in corn. Agron. J. 95, 994–999.

Mamo, M., Malzer, G.L., Mulla, D.J., Huggins, D.R., Strock, J., 2003. Spatial and temporal variation in economically optimum nitrogen rate for corn. Agron. J. 95, 958–964.

Miao, Y., Stewart, B.A., Zhang, F., 2011. Long-term experiments for sustainable nutrient management in China. A review. Agron. Sustain. Devel. 31, 397–414. https://doi.org/10.1051/agro/2010034.

Moebius-Clune, B., Van Es, H., Melkonian, J., 2013. Adapt-N uses models and weather data to improve nitrogen management for corn. Better Crops 97, 7–9.

Morari, F., Zanella, V., Gobbo, S., Bindi, M., Sartori, L., Pasqui, M., Mosca, G., Ferrise, R., 2020. Coupling proximal sensing, seasonal forecasts and crop modelling to optimize nitrogen variable rate application in durum wheat. Precis. Agric. 22, 75–98. https://doi.org/10.1007/s11119-020-09730-6.

Paz, J.O., Batchelor, W.D., Babcock, B.A., Colvin, T.S., Logsdon, S.D., Kaspar, T.C., Karlen, D.L., 1999. Model-based technique to determine variable rate nitrogen for corn. Agr. Syst. 61, 69–75.

Pedersen, M.F., Gyldengren, J.G., Pedersen, S.M., Diamantopoulos, E., Gislum, R., Styczen, M.E., 2021. A simulation of variable rate nitrogen application in winter wheat with soil and sensor information – An economic feasibility study. Agr. Syst. 192, 103147 https://doi.org/10.1016/j.agsy.2021.103147.

Pedersen, S.M., Pedersen, M.F., Ørum, J.E., Fountas, S., Balafoutis, A.T., van Evert, F.K., van Egmond, F., Knierim, A., Kernecker, M., Mouazen, A.M., 2020. Economic, environmental and social impacts. In: Castrignano, A., Buttafuoco, G., Khosla, R., Mouazen, A., Moshou, D., Naud, O. (Eds.), Agricultural Internet of Things and Decision Support for Precision Smart Farming. Elsevier, pp. 279–330.

Peng, S., Buresh, R.J., Huang, J., Yang, J., Zou, Y., Zhong, X., Wang, G., Zhang, F., 2006. Strategies for overcoming low agronomic nitrogen use efficiency in irrigated rice systems in China. Field Crop Res 96, 37–47. https://doi.org/10.1016/j.fcr.2005.05.004.

Peng, S., Buresh, R.J., Huang, J., Zhong, X., Zou, Y., Yang, J., Wang, G., Liu, Y., Hu, R., Tang, Q., Cui, K., Zhang, F., Dobermann, A., 2010. Improving nitrogen fertilization in rice by sitespecific N management. A review. Agronomy Sustain. Devel. 30, 649–656. https://doi.org/10.1051/agro/2010002.

Pierce, F.J., Nowak, P., 1999. Aspects of precision agriculture. Adv. Agron. 67, 1–85.

Ransom, C.J., Kitchen, N.R., Camberato, J.J., Carter, P.R., Ferguson, R.B., Fernández, F. G., Franzen, D.W., Laboski, C.A.M., Nafziger, E.D., Sawyer, J.E., Scharf, P.C., Shanahan, J.F., 2020. Corn nitrogen rate recommendation tools' performance across eight US midwest corn belt states. Agron. J. 112, 470–492. https://doi.org/10.1002/agj2.20035.

Rasmussen, C.E., Williams, C.K.I., 2006. Gaussian processes for machine learning, (Vol. 2):. MIT press Cambridge, MA.

Raun, W.R., Solie, J.B., Johnson, G.V., Stone, M.L., Mullen, R.W., Freeman, K.W., Thomason, W.E., Lukina, E.V., 2002. Improving nitrogen use efficiency in cereal grain production with optical sensing and variable rate application. Agron. J. 94, 815–820.

Raun, W.R., Solie, J.B., Stone, M.L., Martin, K.L., Freeman, K.W., Mullen, R.W., Zhang, H., Schepers, J.S., Johnson, G.V., 2005. Optical sensor-based algorithm for crop nitrogen fertilization. Commun. Soil Sci. Plant Anal. 36, 2759–2781. https://doi.org/10.1080/00103620500303988.

Ren, K., Xu, M., Li, R., Zheng, L., Liu, S., Reis, S., Wang, H., Lu, C., Zhang, W., Gao, H., Duan, Y., Gu, B., 2022. Optimizing nitrogen fertilizer use for more grain and less pollution. J. Clean. Prod. 360, 132180 https://doi.org/10.1016/j.jclepro.2022.132180.

Schoups, G., Vrugt, J.A., 2010. A formal likelihood function for parameter and predictive inference of hydrologic models with correlated, heteroscedastic, and non-Gaussian errors. Water Resour. Res. 46, W10531. https://doi.org/10.1029/2009wr008933.

Solie, J.B., Raun, W.R., Whitney, R.W., Stone, M.L., Ringer, J.D., 1996. Optical sensor based field element size and sensing strategy for nitrogen application. Trans. ASAE 39, 1983–1992.

Stanford, G., 1973. Rationale for optimum nitrogen fertilization in corn production. J. Environ. Qual. 2, 159–166.

Vrugt, J.A., Ter Braak, C.J.F., Diks, C.G.H., Robinson, B.A., Hyman, J.M., Higdon, D., 2009. Accelerating Markov chain Monte Carlo simulation by differential evolution with self-adaptive randomized subspace sampling. Int. J. Nonlinear Sci. Numer. Simulat. 10, 273–290.

Wang, X., Miao, Y., Batchelor, W.D., Dong, R., Kusnierek, K., 2021a. Evaluating model-based strategies for in-season nitrogen management of maize using weather data fusion. Agric. For. Meteorol. 308–309 https://doi.org/10.1016/j.agrformet.2021.108564.

Wang, X., Miao, Y., Dong, R., Zha, H., Xia, T., Chen, Z., Kusnierek, K., Mi, G., Sun, H., Li, M., 2021b. Machine learning-based in-season nitrogen status diagnosis and side-dress nitrogen recommendation for corn. Eur. J. Agron. 123, 126193 https://doi.org/10.1016/j.eja.2020.126193.

Wang, D., Struik, P.C., Liang, L., Yin, X., 2023a. Enhancing field-level forecasting of crop growth status by incorporating the analytically estimated system uncertainties into a data assimilation procedure. Authorea. https://doi.org/10.22541/au.170111043.37713869/v1.

Wang, D., Struik, P.C., Liang, L., Yin, X., 2023b. Estimating leaf and canopy nitrogen contents in major field crops across the growing season from hyperspectral images using nonparametric regression. Authorea. https://doi.org/10.22541/au.170111047.73824045/v1.

Xue, L., Yang, L., 2008. Recommendations for nitrogen fertiliser topdressing rates in rice using canopy reflectance spectra. Biosyst. Eng. 100, 524–534. https://doi.org/10.1016/j.biosystemseng.2008.05.005.

Yao, Y., Miao, Y., Huang, S., Gao, L., Ma, X., Zhao, G., Jiang, R., Chen, X., Zhang, F., Yu, K., Gnyp, M.L., Bareth, G., Liu, C., Zhao, L., Yang, W., Zhu, H., 2012. Active canopy sensor-based precision N management strategy for rice. Agron. Sustain. Dev. 32, 925–933. https://doi.org/10.1007/s13593-012-0094-9.

Yin, X., Goudriaan, J., Lantinga, E.A., Vos, J., Spiertz, H.J., 2003. A flexible sigmoid function of determinate growth. Ann. Bot. 91, 361–371. https://doi.org/10.1093/aob/mcg029.

Yin, X., van Laar, H.H., 2005. Crop systems dynamics: an ecophysiological simulation model for genotype-by-environment interactions. Wageningen Academic Publishers, Wageningen, the Netherlands.

Yu, C., Huang, X., Chen, H., Godfray, H.C.J., Wright, J.S., Hall, J.W., Gong, P., Ni, S., Qiao, S., Huang, G., Xiao, Y., Zhang, J., Feng, Z., Ju, X., Ciais, P., Stenseth, N.C., Hessen, D.O., Sun, Z., Yu, L., Cai, W., Fu, H., Huang, X., Zhang, C., Liu, H., Taylor, J., 2019. Managing nitrogen to restore water quality in China. Nature 567, 516–520. https://doi.org/10.1038/s41586-019-1001-1.

Zhang, F., Wang, J., Zhang, W., Cui, Z., Ma, W., Chen, X., Jiang, R., 2008. Nutrient use efficiencies of major cereal crops in China and measures for improvement. Acta Pedol. Sin. 45, 915–924.
Zhang, F., Chen, X., Vitousek, P., 2013. Chinese agriculture: An experiment for the world. Nature 497, 33–35.
Zhang, J., Wang, W., Krienke, B., Cao, Q., Zhu, Y., Cao, W., Liu, X., 2021. In-season variable rate nitrogen recommendation for wheat precision production supported by fixed-wing UAV imagery. Precis. Agric. 23, 830–853. https://doi.org/10.1007/s11119-021-09863-2.
Zhang, J., Fu, Z., Zhang, K., Li, J., Cao, Q., Tian, Y., Zhu, Y., Cao, W., Liu, X., 2023. Optimizing rice in-season nitrogen topdressing by coupling experimental and modeling data with machine learning algorithms. Comput. Electron. Agric. 209, 107858 https://doi.org/10.1016/j.compag.2023.107858.